

VLBA Radio Observation of J1035-201, J1045-294 and J1046-293

Rishi Mandal, Christina Mester, Eddie Schlafly
Stanford University

Abstract

Radio observations of J1035-201, J1045-294, and J1046-293 were taken in order to characterize their structure on the parsec scale relative to their structure on the kiloparsec scale. All three sources were found to have jets on the kiloparsec scale, while only two exhibited this feature on the parsec scale. For each source, the peak core flux density at the kiloparsec scale was determined to originate almost entirely from a single pointlike source at the parsec scale. The possibility that these sources are black holes was explored and the characteristics of these potential black holes were approximated.

Introduction

Intense, pointlike radio sources, often accompanied by jets, have been found to exist at the center of some galaxies. These sources are known as quasars. It is hypothesized that these radio sources are supermassive black holes. The intense radio emission is thought to be radiated by matter falling into the black hole from a rapidly spinning accretion disk surrounding the black hole. The direction of the accompanying jet of radiation is believed to be parallel to the axis of rotation of the accretion disk. The size of these black holes, according to theory, is expected to be on the parsec scale. Thus, ideally, observations of these sources would be performed at the parsec scale. The Very Large Baseline Array (VLBA) provides this resolution, and so is ideally suited to probing the structure of these sources.

Methods

Three sources with jets at the kiloparsec scale were identified for analysis, using data from the Very Large Array Telescope (VLA).

On 3 April 2005, 0330-0730 UT, these sources were observed using the VLBA. The data that were collected consisted of phase and amplitude measurements over time from the ten different telescopes. These sources were observed at 8.4075 GHz and 8.4155 GHz, with left and right circular polarizations. The measurements were then correlated to synthesize data for the 45 possible baselines.

Before this data can be used to create an image, it must be calibrated. *AIPS* was used to perform this calibration. In order to produce a final image, data from the 16 different channels must be averaged to one well-calibrated channel. Before the channels can be averaged, several adjustments must be made to the data. First, data was adjusted to account for loss in gain due to two-bit sampling used by the VLBA. Next, gain correction is performed. According to the equation,

$$S = \rho_{ij} \sqrt{\frac{T_i^{\text{sys}}}{k_i} \cdot \frac{T_j^{\text{sys}}}{k_j}}$$

where S is source flux, ρ is correlation coefficient, T is temperature and k is the gain of a

given antenna, the gains of the different baselines may vary. In gain correction, this variation is removed. Next, fringe fitting is performed. Imperfect delays in the interferometer cause phase differences among the different channels. This manifests itself as a slope in the phase plot. This slope is removed in this step of the calibration. Bandpass calibration is the next step. By observing a strong known source, 3C279, the data is adjusted to account for filter rolloff on both edges of the graph of amplitude versus frequency. Next, the amplitudes of the radiation for each baseline are compared with measurements of 3C279, so that the amplitudes can be converted to Janskys from meaningless, uncalibrated units. The data can now be averaged to obtain a single channel.

Difmap was then used to synthesize an image from the calibrated data. First, the left-left and right-right polarizations were averaged to obtain a better signal-to-noise ratio. Next, bad data points were removed from graphs of amplitude versus time (tplot), and amplitude versus UV radius (uvplot). Subsequently the images were analyzed and potential point sources selected for cleaning (mapl). This was done by repeatedly using the *clean* and *selfcal* commands until the variance of the noise approached one. Finally, a contour plot of the source flux density was produced. This process was repeated for each source.

These contour plots are shown in Figures 1 through 3 (attached).

Results

Analysis of the contour plots allowed the determination of the peak beam intensity, noise, total flux density (S), jet length and jet position angle. Comparison with the VLA data of the sources yielded peak VLA beam intensity and VLA position angle. These data are reproduced in Table 1.

Table 1: VLBA measurements in comparison with VLA measurements for the three observed sources.

<i>Source</i>	<i>Peak_{VLBA}</i> (Jy/beam)	<i>Rms noise</i> (mJy/beam)	<i>S_{VLBA}</i> (mJy)	<i>Peak_{VLA}</i> (mJy)	<i>Fraction</i> (%)	<i>Jet Length</i> (pc)	<i>Jet Position Angle</i> (degrees)	<i>Delta PA</i> (VLBA – VLA) (degrees)
<i>J1035-201</i>	.869	.44	1230	1214	101	187	210	60
<i>J1045-294</i>	.0754	.48	253	266	95	118	270	-20
<i>J1046-293</i>	.0361	.30	33	35	94	No jet	n/a	n/a

Using the redshift values¹, the number of parsecs per milliarcsecond was calculated². This was used to determine jet length in parsecs (Table 2).

¹ Obtained using Nasa's Extragalactic Database (NED)

² Using Ned Wright's Cosmological Calculator. <http://www.astro.ucla.edu/~wright/cosmocalc.html>

Table 2: Redshift values and jet lengths for the three observed sources.

<i>Source</i>	<i>Redshift</i>	<i>Jet Length (mas)</i>	<i>Jet Length (pc)</i>
<i>J1035-201</i>	2.198	22	187
<i>J1045-294</i>	2.128	14	118
<i>J1046-293</i>	0.0598	No jet	No jet

Discussion & Conclusion

Each of the three observed sources was active in the radio band. Consistent with the expectations from the VLA data, two sources, J1035-201 and J1045-294, exhibited jets on the milliarcsecond scale. However, the third source, J1046-293, did not have a jet on this scale.

There were significant differences in the position angles of the jets between the VLA kiloparsec-scale images and the VLBA parsec-scale images. One possible explanation of this is that the jet may be physically redirected due to collision with some astronomical object. A more plausible explanation requires that the quasar's jet be angled nearly directly toward the telescope. At this angle, small variations in jet direction can result in large difference in jet position angle.

This explanation is particularly likely because of the absence of detectable counterjets in the images. Symmetry suggests that counterjets should be present. However, if one jet is positioned directly toward the telescope, then its radiation would be Doppler-boosted to high energy, and would therefore be very intense. The counterjet's radiation, however, would be Doppler-boosted in the opposite direction, and would therefore be difficult to detect.

Additionally, this explanation accounts for the rareness of objects that have both observable jets and counterjets. Any jet positioned away from the telescope would not have its radiation Doppler-boosted to high energy toward the telescope, and so would be relatively difficult to observe. Moreover, radiation from the jets is expected to be highly directional, so most of the radiation from jets not positioned toward the telescope would not be observed.

The total VLBA flux density accounted for approximately 100% of the peak VLA flux density. This suggests that most of the peak VLA radiation, potentially coming from an entire galaxy, actually originates from the single, central point sources observed by the VLBA.

If the radio sources are in fact massive black holes, the radius of the black holes can be estimated. To accomplish this, the luminosity of the sources must be determined. Luminosity is related to apparent magnitude by the equation:

$$m = -2.5 \cdot \log\left(\frac{L}{4\pi D_L^2}\right) + c$$

where m is apparent magnitude, L is luminosity, D_L is luminosity distance and c is a

constant. This gives:

$$m - m_{sun} = -2.5 \cdot \log \left[\frac{L}{L_{sun}} \cdot \left(\frac{10 pc}{D_L} \right)^2 \right].$$

Solving for luminosity, the following equation is obtained:

$$\left(\frac{L}{L_{sun}} \right) = \left(\frac{D_L}{10 pc} \right)^2 \cdot 10^{0.4(m_{sun} - m)}.$$

Using apparent magnitudes³ and luminosity distances⁴, the following table of luminosities was produced (Table 3).

Table 3: A table summarizing luminosities of the three observed sources. Luminosity is given in solar masses.

<i>Source</i>	<i>Redshift</i>	<i>Luminosity distance (D_L) (Mpc)</i>	<i>Apparent Magnitude (m)</i>	<i>Luminosity (L_{sun})</i>
<i>J1035-201</i>	2.198	17674.7	17.3	$3.1 * 10^{13}$
<i>J1045-294</i>	2.128	16984.3	18.6	$8.7 * 10^{12}$
<i>J1046-293</i>	0.0598	264.3	16.0	$2.3 * 10^{10}$

The Eddington luminosity is the maximum luminosity that a black hole of a particular mass can have. By supposing that the sources are actually radiating at this maximum Eddington luminosity, an approximate lower bound on the mass of the hypothesized black holes can be obtained.

Eddington luminosity is given by:

$$L_{edd} = 10^{38} \cdot \left(\frac{M}{M_{sun}} \right)$$

where M is the mass of the object and M_{sun} is the mass of the sun. Solving for the mass of the object and changing units to solar luminosities produces the equation:

$$M = (4 \cdot 10^{-5}) \left(\frac{L}{L_{sun}} \right) \cdot M_{sun}.$$

The Schwarzschild radius of a black hole is determined by its mass, according to the equation:

$$R_{sch} = \frac{2GM}{c^2} = (10^{-13} pc) \left(\frac{M}{M_{sun}} \right)$$

where G is the gravitational constant, and c is the speed of light. Using the lower bounds on the masses of the hypothesized black holes calculated by the equation for the Eddington luminosity, lower bounds for the Schwarzschild radius of the black holes can be determined (Table 4).

³ Obtained from NED.

⁴ Using Ned Wright's Cosmological Calculator. <http://www.astro.ucla.edu/~wright/cosmocalc.html>

Table 4: Predicted masses and Schwarzschild radii of the three observed sources.

<i>Source</i>	<i>Mass (M_{sun})</i>	<i>R_{sch} (pc)</i>	<i>Jet Length (R_{sch})</i>
<i>J1035-201</i>	$1.24 \cdot 10^9$	3.1	60.3
<i>J1045-294</i>	$3.48 \cdot 10^8$	0.87	135.6
<i>J1046-293</i>	$9.2 \cdot 10^5$	0.0023	n/a

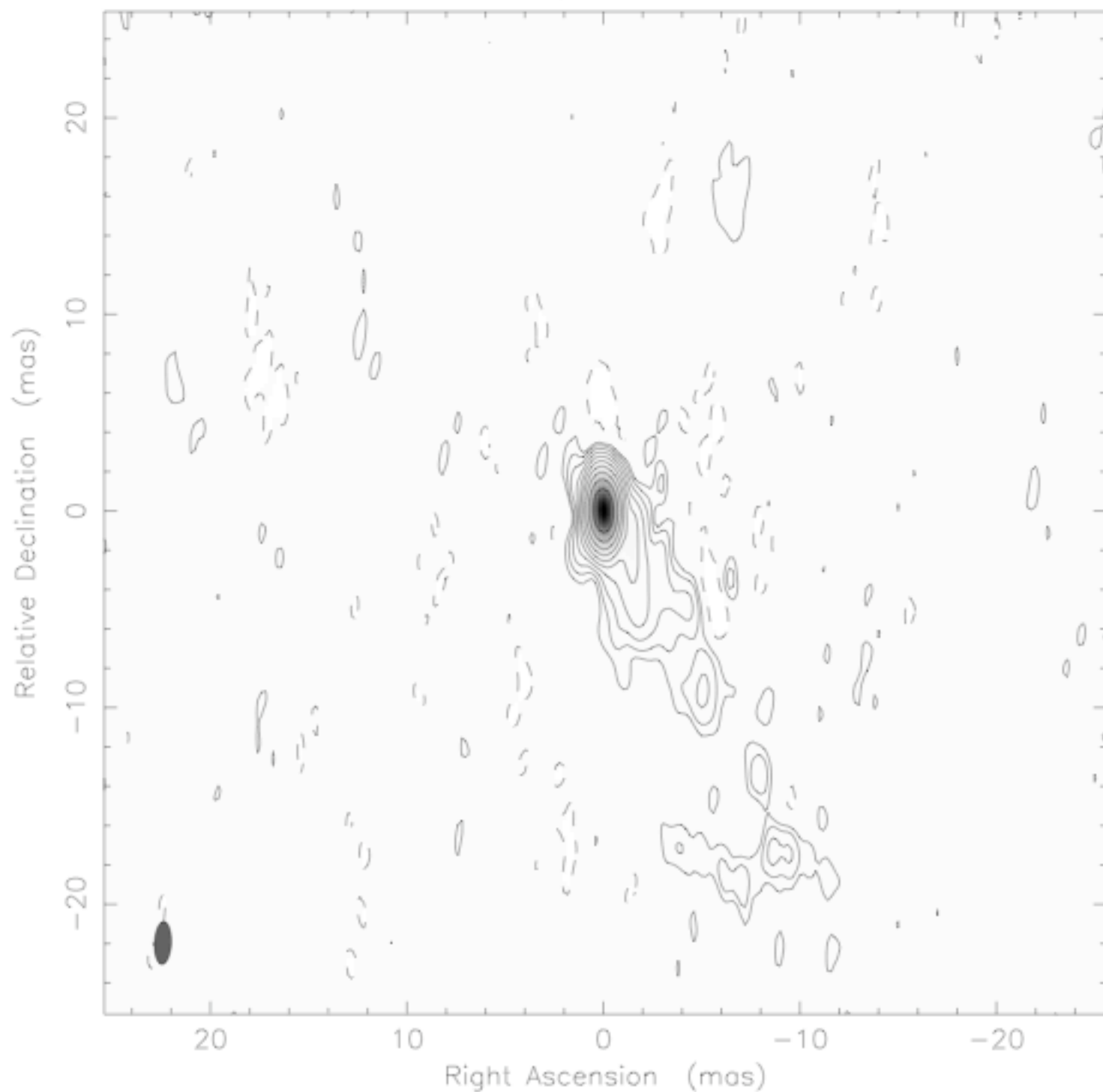
The VLBA has approximately milliarcsecond resolution. For J1035-201 and J1045-294, this corresponds to about 8 parsec resolution. Thus the lower bounds on the Schwarzschild radii of the black holes are found to be about the same order of magnitude as the resolution of the VLBA image. The parsec-scale jets are found to be approximately 10^2 Schwarzschild radii.

There is approximately 0.4 mJy rms noise in each of the three final images. The potential sources for this error include intrinsic noise from the object, background noise, and atmospheric fluctuations that introduce unanticipated phase delays to detected radiation. However, the rms noise is far less than the signal received from the sources and can thus be neglected.

Imperfect calibration of the data may produce systematic errors.

It should be noted that jet lengths presented in Tables 1, 2 and 4 represent the apparent lengths found on the images. The true jet length can only be determined if its angle of incidence is known.

Clean I map. Array: BFHKLMNOPS
J1035-20 at 8.415 GHz 2005 Apr 03



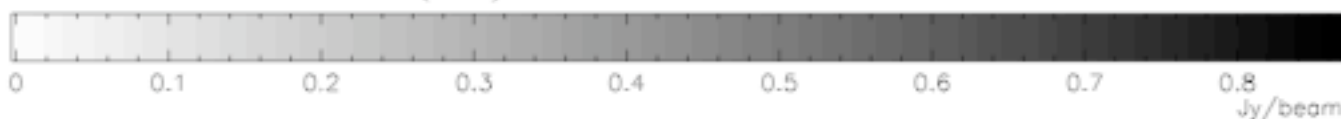
Map center: RA: 10 35 02.155, Dec: -20 11 34.359 (2000.0)

Map peak: 0.869 Jy/beam

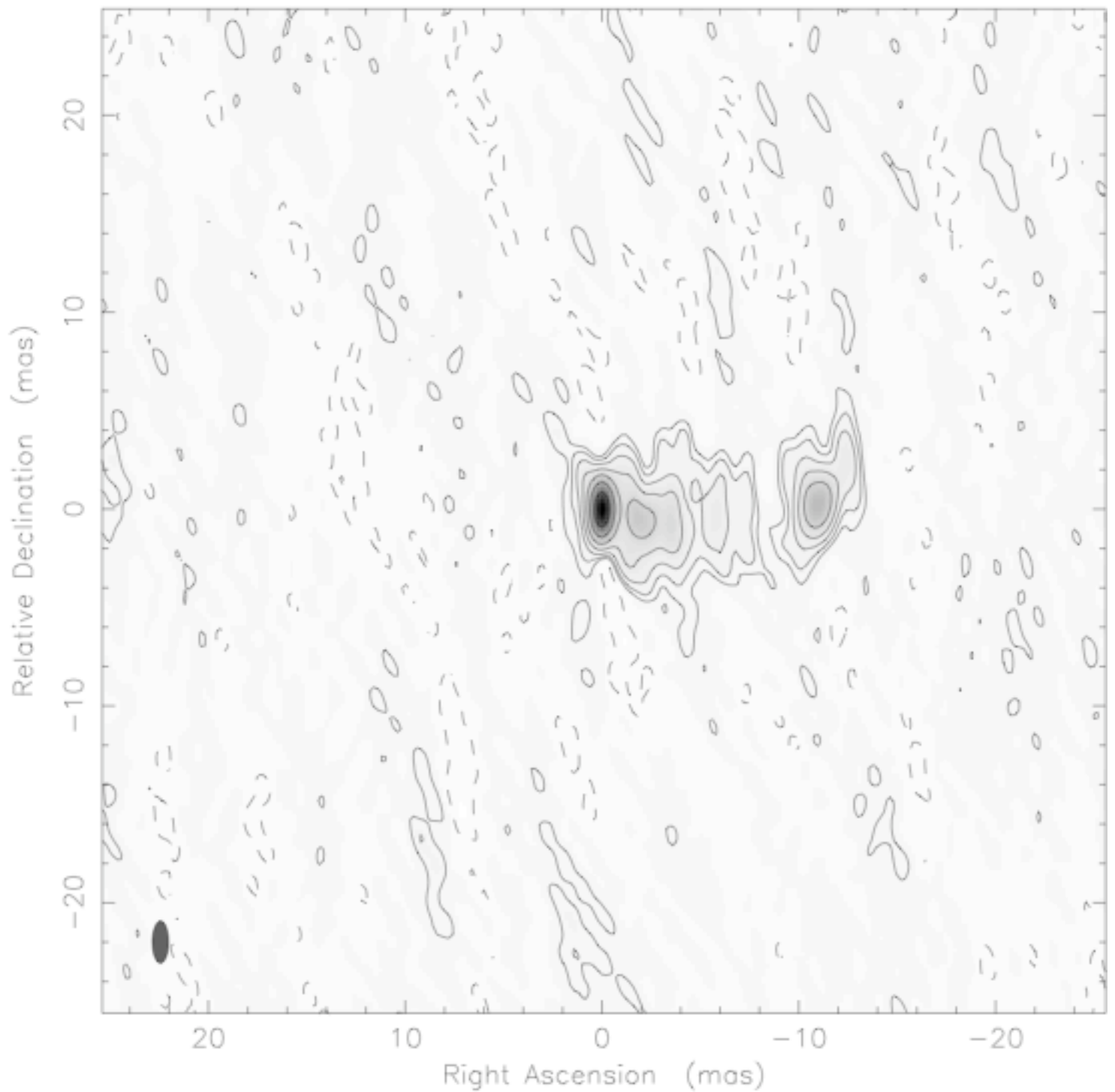
Contours %: -0.1 0.1 0.2 0.4 0.8 1.6 3.2 6.4 12.8

Contours %: 25.6 51.2

Beam FWHM: 2.16 x 0.849 (mas) at -2.73°



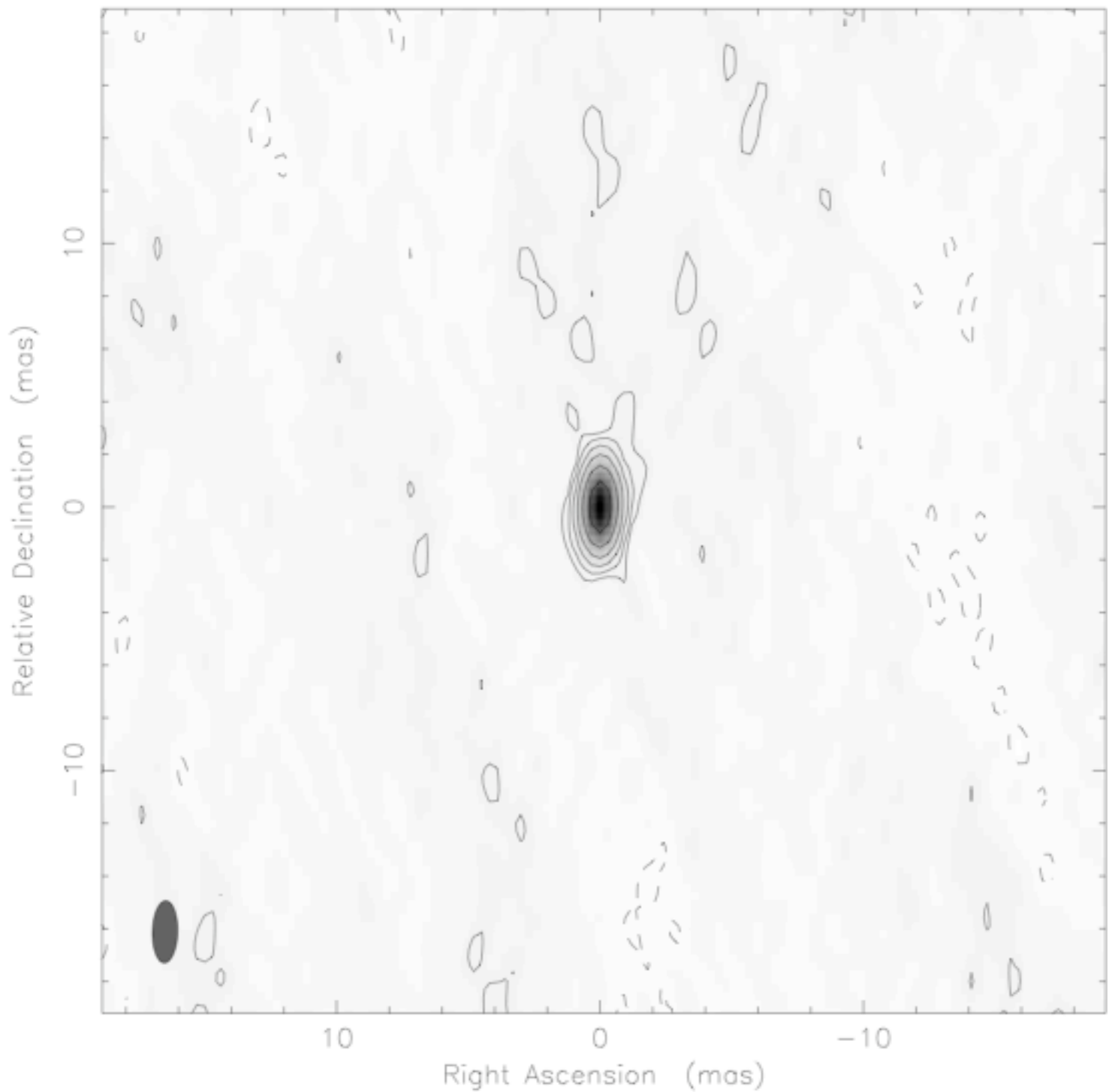
Clean I map. Array: BFHKLMNOPS
J1045-29 at 8.415 GHz 2005 Apr 03



Map center: RA: 10 45 40.620, Dec: -29 27 26.350 (2000.0)
Map peak: 0.0754 Jy/beam
Contours %: -1 1 2 4 8 16 32 64
Beam FWHM: 2.11 x 0.818 (mas) at -0.125°



Clean I map. Array: BFHKLMNOPS
J1046-29 at 8.415 GHz 2005 Apr 03



Map center: RA: 10 46 09.930, Dec: -29 21 09.850 (2000.0)
Map peak: 0.031 Jy/beam
Contours %: -2 2 4 8 16 32 64
Beam FWHM: 2.36 x 0.956 (mas) at -1.48°

